2 1/2-D elastic ray-Born migration/inversion theory for transversely isotropic media

David W.S. Eaton and Robert R. Stewart

ABSTRACT

Linearized (ray-Born) scattering formulae are derived that relate the observed seismic wavefield to perturbations in *qP*- and *qS*-wave velocities, density and the three Thomsen anisotropy parameters (δ, ε and γ) for transversely isotropic media. These formulae form the basis for a $2\text{-}\frac{1}{2}$ dimensional migration/inversion algorithm that accounts for anisotropic effects in both wave propagation and scattering. The technique is applicable to seismic data acquired across geologic strike over a 2-D inhomogeneous medium. The l_2-norm inversion is carried out by minimization of an objective function that incorporates *a priori* data and model covariances, so that the problem is always well-posed and can accommodate insufficient and inaccurate data. Anisotropic model parameters that are obtained in the inversion may be useful for sand/shale discrimination, characterization of thinly laminated rock layers or analysis of fracturing.

INTRODUCTION

Seismic inversion attempts to reconstruct earth parameters using experimental observations, based on some model for wave propagation. Solution to the seismic inverse problem is often difficult because the relationship between measured values and model parameters is generally non-linear. A useful linearized approach stems from the Born approximation, based on an inverse scattering formalism originally developed in quantum physics.

The literature contains numerous examples of this method applied to seismic data. Born-inversion techniques have been developed for constant-density acoustic media (Cohen and Bleistein, 1979; Beylkin, 1985; Miller et al., 1987), variable-density acoustic media (Raz, 1981; Clayton and Stolt, 1981; Weglein et al., 1986; LeBras and Clayton, 1988) isotropic-elastic media (Beydoun and Mendes, 1989; Beydoun et al., 1989, 1990; Beylkin and Burridge, 1990) and fractured media (Tura, 1990). All of these methods linearize the forward problem that relates the scattered wavefield to small perturbations in the medium parameters. An additional high frequency approximation based on ray theory is often invoked in order to permit the use of inhomogeneous reference models (Bleistein and Gray, 1985; Miller et al., 1987; Beydoun and Mendes, 1989; Beylkin and Burridge, 1990).

Methods of performing Born inversion can be divided into two major categories. Asymptotic-direct methods have been developed based on the theory of the inverse generalized Radon transform (Beylkin, 1985; Cohen et al., 1986; Miller et al., 1987, Beylkin and Burridge, 1990). The alternative, indirect approach seeks a solution that minimizes (in the l_2 norm) an objective or cost function (LeBras and Clayton, 1988;

Beydoun and Mendes, 1989). This approach has several advantages over direct-inversion techniques: first, it is more straightforward to incorporate *a priori* information into the inversion, and secondly, insufficient (eg. single component) and inaccurate data can be accommodated in a natural way.

In their implementation, both the direct and indirect methods involve an imaging step that resembles prestack depth migration, followed by an adjoint operation that images the perturbations in the medium parameters using the amplitude-versus-offset information in the observed data. Because of the similarity of the imaging process to classical migration, this technique is often referred to as "migration/ inversion" (M/I) to distinguish it from more general elastic non-linear inversion methods (eg. Tarantola, 1986).

This study will focus on the feasibility of solving for additional anisotropic parameters in the inversion procedure. The model is assumed to be transversely isotropic, the simplest form that anisotropy can take aside from pure isotropy. A single infinite-fold axis of symmetry exists for this symmetry class (Figure 1). The minimum number of parameters needed to describe the medium is six, compared to three for the isotropic case. The three principle causes mechanisms for transverse isotropy in sedimentary rocks are (Crampin et al., 1984):

1) *Lithologic anisotropy* caused by parallel alignment of elongated grains during deposition, particularly in clays and shales;

2) *Periodic thin-layered (PTL) anisotropy* produced by alternating low- and high-velocity layers, and;

3) *Crack-induced anisotropy* caused by a preferred orientation of cracks or fractures due to a present or fossil stress field.

These three causal mechanisms suggest that information obtained about anisotropic parameters for a transversely isotropic medium could be used to help discriminate between sands and shales, identify and characterize thin-layered zones, and infer crack orientation and density. Figures 2 and 3 show scatter plots of anisotropic parameters and α/β for sandstones and shales, based on Thomsen's (1986) compilation of measured anisotropy of sedimentary rocks. These graphs suggest that, in general, shales are more strongly anisotropic than sandstones, although the scatter is large and the data are not adequate to easily delineate trends. One exception appears to be the good correlation between γ and ε (Figure 3b). The data here suggest that the ratio γ/ε is higher for shales than sandstones.

In addition to extending the M/I technique to include transversely isotropic media, this study will explicitly adapt the equations for 2-$\frac{1}{2}$ dimensions using the method of stationary phase. The term "2-$\frac{1}{2}$ D" (Bleistein, 1986; Bleistein et al., 1987) implies that the model is assumed to be invariant in one direction, with

Fig. 1. (next page) Principle causes of transverse isotropy in sedimentary rocks (Crampin et al., 1984). a) Lithologic anisotropy, due to preferred alignment of elongated mineral grains during deposition. b) Periodic thin-layered anisotropy due to alternating low- and high-velocity layers. c) Crack-induced anisotropy, from parallel alignment of open or fluid-filled cracks. Of these, only lithologic anisotropy is intrinsic (ie. independent of wavelength). The other causes depend on averaging of the medium parameters over the seismic wavelength. Normally, the slow direction of wave propagation is parallel to the axis of symmetry.

a)

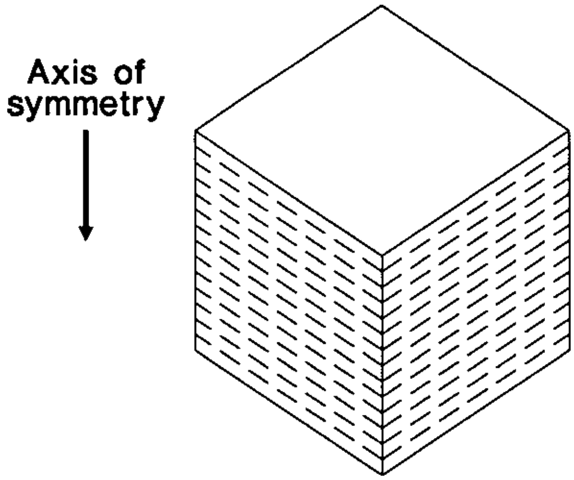

b)

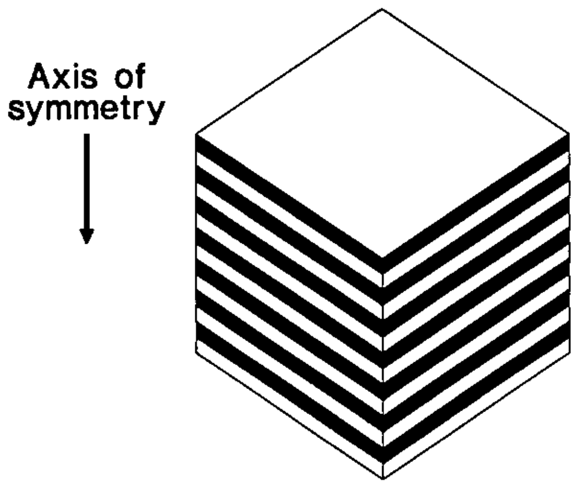

c)

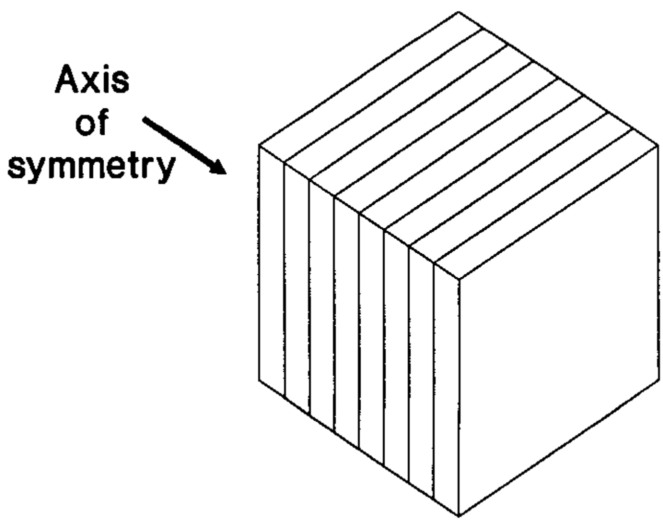

data recorded in the plane of symmetry. This notion arises from the common exploration scemario in which sources and receivers are aligned in a linear, rather than planar, fashion. This approach accounts for 3-D spreading and scattering without calculating full 3-D Green's functions.

RAY-BORN APPROXIMATION

The main aspects of the ray-Born approximation for elastic media are reviewed here, following closely the derivation of Beylkin and Burridge (1990). The frequency-domain elastodynamic Green's tensor (dyadic) for an anisotropic, inhomogeneous 3-D medium satisfies

$$(c_{lmpq}G_{jp,q})_{,m} + \omega^2\rho G_{jl} = -\delta_{jl}\delta(\mathbf{x}-\mathbf{s}) \ , \tag{1}$$

where c_{lmpq} is the 81-component elastic stiffness tensor with symmetry properties $c_{lmpq} = c_{mlpq} = c_{lmqp} = c_{pqlm}$; ρ is density; both c_{lmpq} and ρ are functions of position $\mathbf{x}$; and $G_{jl}(\mathbf{x},\omega;\mathbf{s})$ is the *l*th component of displacement at position $\mathbf{x}$ due to a source in the *j*-direction at position $\mathbf{s}$. In addition, δ_{jl} is the Kronecker symbol, $\delta(\xi)$ is the dirac delta, Einstein's summation convention for repeated indices is used and a comma implies spatial differentiation.

The first step in the procedure is to split the medium parameters and Green's tensor into two parts,

$$c_{lmpq} = c^0_{lmpq} + c'_{lmpq} \ , \tag{2}$$

$$\rho = \rho^0 + \rho' \ , \tag{3}$$

and

$$G_{jl} = G^0_{jl} + U_{jl} \ , \tag{4}$$

where c^0_{lmpq} and ρ^0 are the stiffnesses and density of the reference medium, and $G^0_{jl}(\mathbf{x},\omega;\mathbf{s})$ satisfies

$$(c^0_{lmpq}G^0_{jp,q})_{,m} + \rho^0\omega^2 G^0_{jl} = -\delta_{jl}\delta(\mathbf{x}-\mathbf{s}) \ . \tag{5}$$

c'_{lmpq} and ρ' represent small perturbations from the reference parameters, and U_{jl} is the *scattered* wavefield (ie. the part of the total wavefield that is not accounted for

Fig. 2. (next page) a) Scatter plot of measured values of ε vs. α/β for sandstones (squares) and argillaceous rocks (crosses) from Table 1 in Thomsen (1986). Average sandstone and shale values are circled. b) Scatter plot of δ vs. α/β for same rocks. c) Scatter plot of γ vs α/β for same rocks.

Fig. 3. (page after next) a) Scatter plot of δ vs. ε for sandstones (squares) and shales (crosses) for same rocks as Figure 2. The poor correlation between δ and ε implies that elliptical anisotropy is uncommon (see Thomsen, 1986). b) Scatter plot of γ vs. ε for same rocks. These data show better correlation and suggest that $(\gamma/\varepsilon)_{shale} > (\gamma/\varepsilon)_{sand}$. c) Scatter plot of δ vs. γ for same rocks.

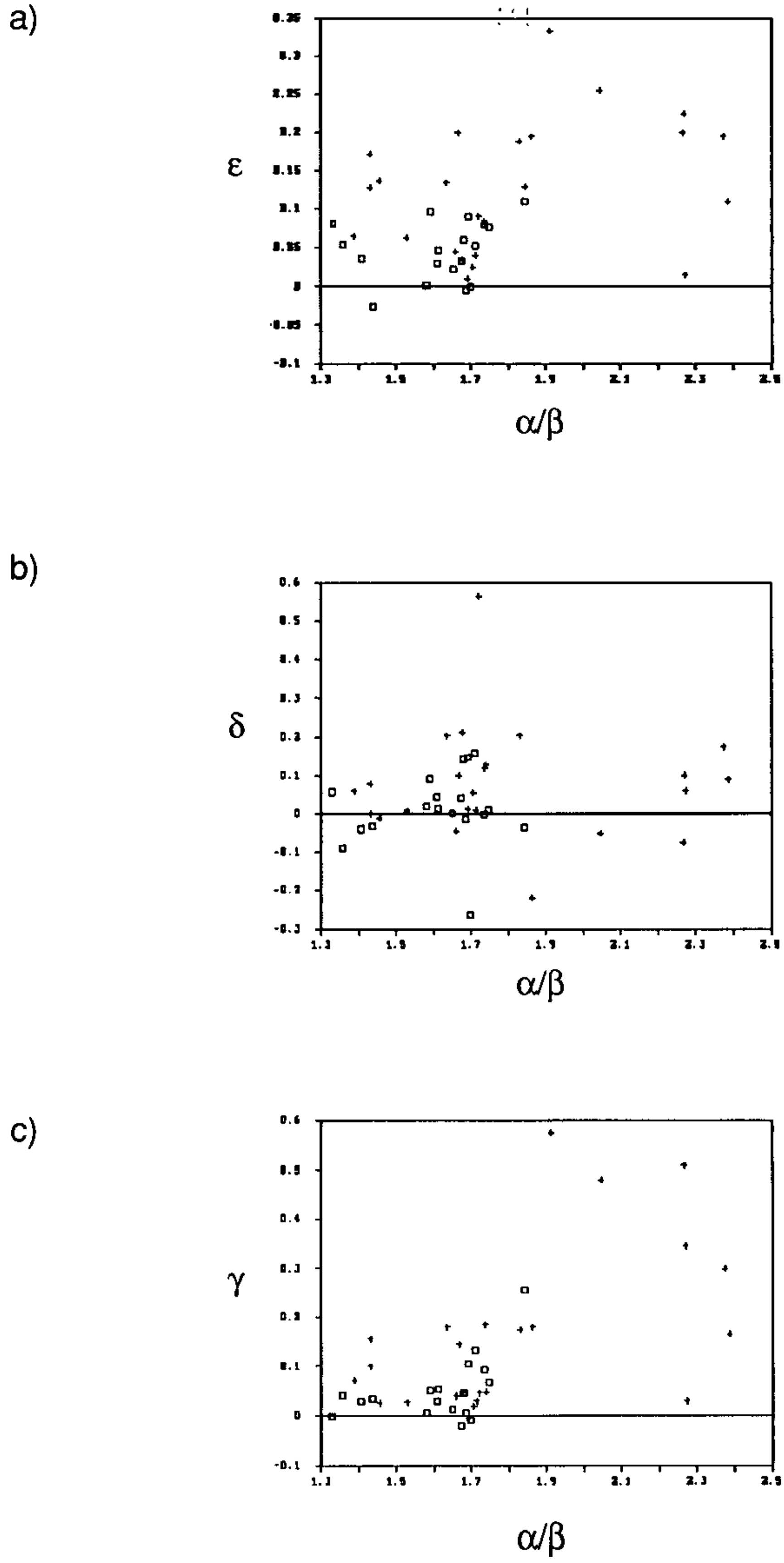

FIGURE 2

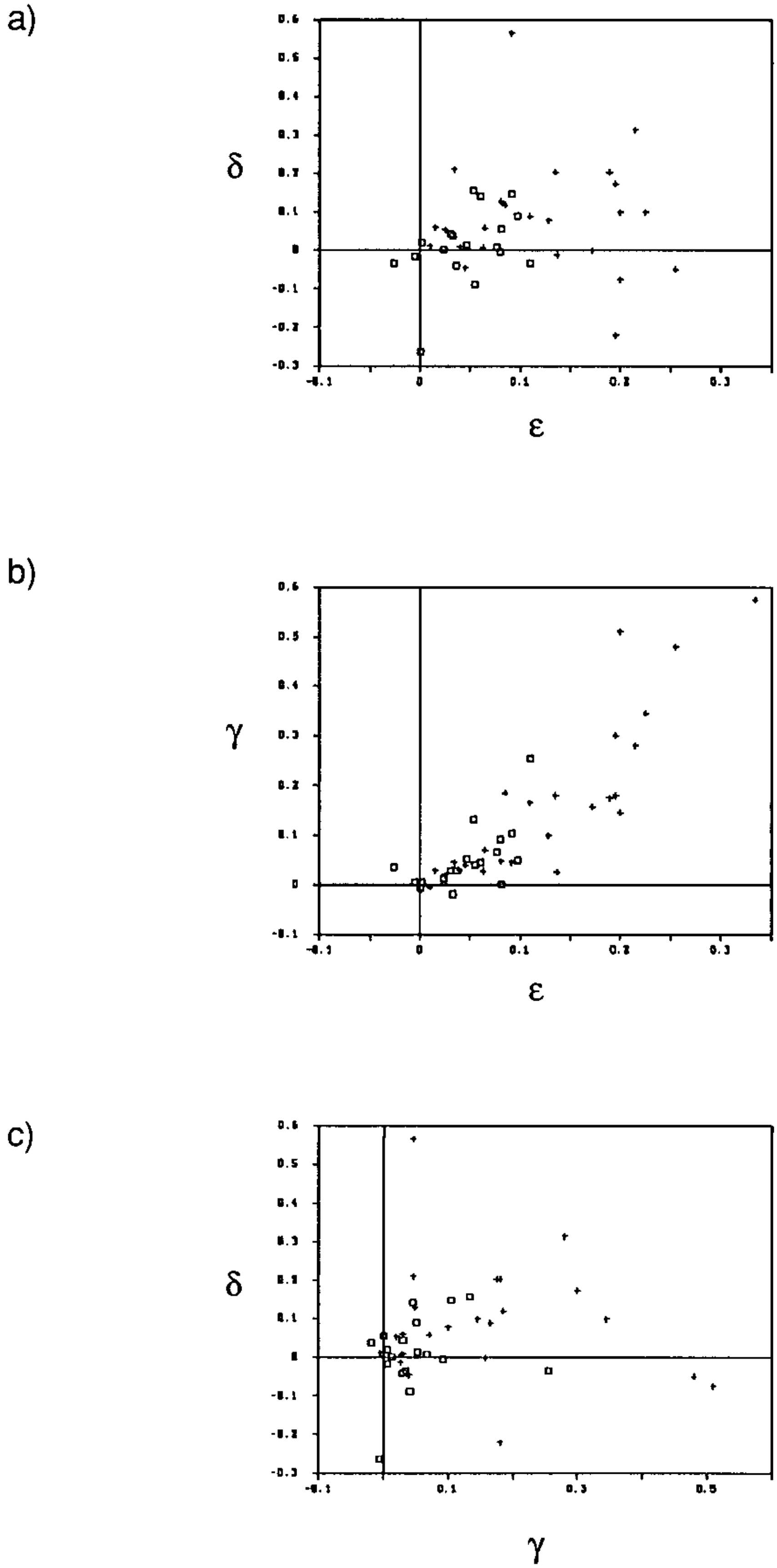

FIGURE 3

by the reference Green's tensor). Subtracting equation (5) from equation (1) gives

$$(c^0_{lmpq}U_{jp,q})_{,m} + \rho^0\omega^2 U_{jl} = -(c'_{lmpq}G_{jp,q})_{,m} - \rho'\omega^2 G_{jl} \ . \tag{6}$$

The parameters on the left side of equation (6) belong to the reference medium, while the right side plays the role of body sources. Therefore, U_{jl} may be expressed as a spatial convolution of the source term with the reference Green's function,

$$U_{jk}(\mathbf{r},\omega;\mathbf{s}) = \int_D d\mathbf{x} G^0_{lk}(\mathbf{r},\omega;\mathbf{x})[c'_{lmpq}G_{jp,q}(\mathbf{x},\omega;\mathbf{s})]_{,m} + G^0_{lk}(\mathbf{r},\omega;\mathbf{x})\rho'\omega^2 G_{jl}(\mathbf{x},\omega;\mathbf{s}) \ . \tag{7}$$

As noted by Clayton and Stolt (1981) for the acoustic case, this expression differs from quantum scattering theory, since it involves spatial derivatives of the medium parameters. However, if the domain D containing nonzero c'_{lmpq} and ρ' is finite, then equation (7) can be simplified by integrating the terms involving c'_{lmpq} by parts, since the boundary terms vanish (Beylkin and Burridge, 1990). Hence, equation (7) may be rewritten

$$U_{jk}(\mathbf{r},\omega;\mathbf{s}) = \int_D d\mathbf{x} G^0_{lk,m}(\mathbf{r},\omega;\mathbf{x})c'_{lmpq}G_{jp,q}(\mathbf{x},\omega;\mathbf{s}) + G^0_{lk}(\mathbf{r},\omega;\mathbf{x})\rho'\omega^2 G_{jl}(\mathbf{x},\omega;\mathbf{s}) \ . \tag{8}$$

Note that equation (8) is exact but non-linear for G'_{jk}. However, if the perturbations c'_{lmpq} and ρ' are small, then

$$G_{jl}(\mathbf{x},\omega;\mathbf{s}) \approx G^0_{jl}(\mathbf{x},\omega;\mathbf{s}) \ . \tag{9}$$

Making this substitution into equation (8) yields the (first) Born approximation,

$$U_{jk}(\mathbf{r},\omega;\mathbf{s}) \approx \int_D d\mathbf{x} G^0_{lk,m}(\mathbf{r},\omega;\mathbf{x})c'_{lmpq}G^0_{jp,q}(\mathbf{x},\omega;\mathbf{s}) + G^0_{lk}(\mathbf{r},\omega;\mathbf{x})\rho'\omega^2 G^0_{jl}(\mathbf{x},\omega;\mathbf{s}) \ . \tag{10}$$

To obtain a more formal series solution, rewrite equation (7) in operator notation,

$$U = G^0VG \ , \tag{11}$$

where the operator V represents the scattering potential, and is given by

$$V = \left[c'_{lmpq,m} + c'_{lmpq}\frac{\partial}{\partial x_m} + \omega^2\rho'\right] \ . \tag{12}$$

Adding G^0 to both sides of equation (11) gives the Lippmann-Schwinger equation,

$$G = G^0 + G^0VG \ , \tag{13}$$

for which the solution is well known:

$$G = (I - G^0V)^{-1}G^0 \ . \tag{14}$$

The operator $(I-G^0V)^{-1}$ can be expanded as a power series (the Born series),

$$(I-G^0V)^{-1} = \sum_{k=0}^{\infty}(G^0V)^k \ . \tag{15}$$

Truncation of the Born series after the k=1 term represents the first Born approximation. Higher-order Born approximations are also possible in seismic applications (Snieder, 1990).

A zeroth-order ray approximation to the elastodynamic Green's tensor, representing the direct qP and $qS1$ and $qS2$ waves may be written

$$\Gamma^0_{kl}(\mathbf{x},\omega;\mathbf{s}) = A^P\tilde{e}^3_l(\mathbf{x})\tilde{e}^3_k(\mathbf{s})e^{i\omega\tau P} + A^{S1}\tilde{e}^1_l(\mathbf{x})\tilde{e}^1_k(\mathbf{s})e^{i\omega\tau S1} + A^{S2}\tilde{e}^2_l(\mathbf{x})\tilde{e}^2_k(\mathbf{s})e^{i\omega\tau S2} \ . \tag{16}$$

This expression is patterned after the equivalent expression for the isotropic case (Beydoun and Mendes, 1989). The notation Γ^0_{kl} is used to distinguish the high-frequency approximate Green's tensor from the exact Greens tensor, G^0_{kl}. By convention, the $S1$ arrival is associated with the shearwave that is polarized in the SV sense (approximately), and the $S2$ arrival is associated with the shearwave polarized in the SH sense. Since only one arrival for each wave type is accounted for, the expression is valid only when the wave sheets do not contain cusps or triplications (see Musgrave, 1970). This restriction limits the range of anisotropic behaviour that can be analyzed, but is much less restrictive than, for example, the assumption of elliptical anisotropy.

The unit eigenvectors $\tilde{\mathbf{e}}^1$, $\tilde{\mathbf{e}}^2$ and $\tilde{\mathbf{e}}^3$ form the ray-centred co-ordinate system (Cerveny, 1985) for the isotropic case, where $\tilde{\mathbf{e}}^3$ is parallel to the ray and $\tilde{\mathbf{e}}^1$ and $\tilde{\mathbf{e}}^2$ are in the plane of the wavefront (Figure 4). In general, however, $\tilde{\mathbf{e}}^1$, $\tilde{\mathbf{e}}^2$ and $\tilde{\mathbf{e}}^3$ are unit particle-motion polarization vectors and are not orthogonal. The amplitude terms $A^P(\mathbf{x},\mathbf{s})$, $A^{S1}(\mathbf{x},\mathbf{s})$ and $A^{S2}(\mathbf{x},\mathbf{s})$ and traveltimes $\tau^P(\mathbf{x},\mathbf{s})$, $\tau^{S1}(\mathbf{x},\mathbf{s})$ and $\tau^{S2}(\mathbf{x},\mathbf{s})$ satisfy the corresponding transport and eikonal equations in the ray-centred co-ordinate system (Cerveny, 1985). In addition, the amplitude terms are chosen to satisfy the boundary conditions at interfaces.

The Green's function for the scattered direct arrival may be written in a similar fashion,

$$\Gamma^0_{kl}(\mathbf{r},\omega;\mathbf{x}) = A^P\hat{e}^3_l(\mathbf{r})\hat{e}^3_k(\mathbf{x})e^{i\omega\tau P} + A^{S1}\hat{e}^1_l(\mathbf{r})\hat{e}^1_k(\mathbf{x})e^{i\omega\tau S1} + A^{S2}\hat{e}^2_l(\mathbf{r})\hat{e}^2_k(\mathbf{x})e^{i\omega\tau S2} \ . \tag{17}$$

The superscript ~ is used to denote the direct arrival from the source, and the superscript ^ is used for scattered direct arrival. The leading singular term in the spatial derivatives of equation (16) may be written (Beylkin and Burridge, 1990)

$$\begin{aligned}\Gamma^0_{kl,m}(\mathbf{x},\omega;\mathbf{s}) = {} & i\omega\tau^P_{,m}A^P\tilde{e}^3_l(\mathbf{x})\tilde{e}^3_k(\mathbf{s})e^{i\omega\tau P} + i\omega\tau^{S1}_{,m}A^{S1}\tilde{e}^1_l(\mathbf{x})\tilde{e}^1_k(\mathbf{s})e^{i\omega\tau S1} \\ & + i\omega\tau^{S1}_{,m}A^{S2}\tilde{e}^2_l(\mathbf{x})\tilde{e}^2_k(\mathbf{s})e^{i\omega\tau S2} \ .\end{aligned} \tag{18}$$

The expression for the spatial derivative of the scattered Green's function (equation (17)) is very similar.

Note that for the direct arrival from the source,

$$\tilde{\alpha}\tau^P_{,m} = \tilde{n}_m \ \text{ and } \ \tilde{\beta}\tau^S_{,m} = \tilde{n}_m \ , \tag{19}$$

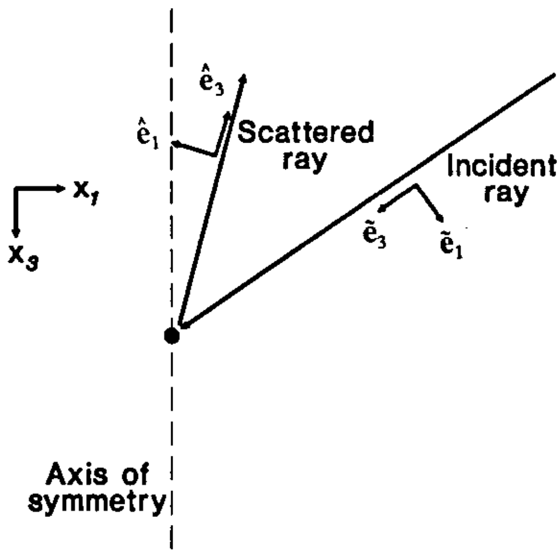

Fig. 4. Ray geometry for incident and scattered rays, showing unit eigenvectors.

where $\tilde{\alpha}$ and $\tilde{\beta}$ are the reference qP- and qS-wave phase velocities in the direction of propagation, and $\tilde{\mathbf{n}}$ is the unit normal vector to the wavefront. For the scattered direct arrival,

$$\hat{\alpha}\tau^{P}{}_{,m} = -\hat{n}_m \quad \text{and} \quad \hat{\beta}\tau^{S}{}_{,m} = -\hat{n}_m \quad . \tag{20}$$

Substituting the approximate Green's tensor, along with (19) and (20) into the Born formula (10), the scattering equation for an incident wave type (i) and a scattered wave type (s) can be written for a specific parameter linearizaion (q) as

$$U^{is}_{jk} \approx -\omega^2 \int_D \mathrm{d}\Omega \, L^q_{lp} s^{is}_l(\mathbf{x}) \delta m^q_p A(\mathbf{r},\mathbf{x},\mathbf{s}) C_{jk}(\mathbf{r},\mathbf{x},\mathbf{s}) e^{i\omega\tau(r,x,s)} \quad . \tag{21}$$

The vector $\mathbf{s}^{is}(\mathbf{x})$ and the parameter linearization matrix L^q_{lp} govern the amplitude radiation pattern. $\delta\mathbf{m}$ is the model parameter vector, $A(\mathbf{r},\mathbf{x},\mathbf{s})$ is the total geometrical spreading term and $C(\mathbf{r},\mathbf{x},\mathbf{s})$ represents the ray coupling with the source and receiver. These are defined for specific incident and scattered waves below.

2-½ D STATIONARY PHASE APPROXIMATION

We now specialize the analysis to the following case:

1) the medium has transversely isotropic symmetry or higher (the structure of the elastic stiffness tensor is discussed below);

2) medium parameters do not vary in the direction normal to the plane containing sources and receivers (the sagittal plane), given by $x_2 = 0$;

3) the anisotropic axis of symmetry lies in the sagittal plane.

Under these conditions, the two qS waves are decoupled and qP waves are coupled only with $qS1$ waves (for rays within the sagittal plane), thus allowing the scattering formulae to be considerably simplified. In addition, these conditions imply that $\tau_{,2}|_{x2=0} = 0$.

For x_1 and x_3 fixed, and for large ω, $e^{i\omega\tau}$ will oscillate very rapidly as a function of x_2, and the principal contribution will occur in the vicinity of the point of stationary phase (x_2=0). Equation (21) may then be rewritten

$$U_{jk}^{is} \approx -\omega^2 \int\int_{D'} dx_1 dx_3\, L_{lp}^q s_l^{is}(\mathbf{x})\delta m_p^q A(\mathbf{r},\mathbf{x},\mathbf{s}) C_{jk}(r,x,s) \int dx_2 e^{i\omega\tau(r,x,s)} \quad , \tag{22}$$

where domain D′ is the cross-sectional area of domain D in the x_1-x_3 plane, and **L**, **s**, A and **C** are evaluated at x_2=0. The Taylor expansion for τ about the point of stationary phase may be written

$$\tau(x_2) = \tau(0) + x_2^2\tau_{,22}/2|_0 \ , \tag{23}$$

ignoring third and higher-order terms. Substituting (23) into equation (22) gives

$$U_{jk}^{is} \approx -\omega^2 \int\int_{D'} dx_1 dx_3\, L_{lp}^q s_l^{is}(\mathbf{x})\delta m_p^q A(\mathbf{r},\mathbf{x},\mathbf{s}) C_{jk}(\mathbf{r},\mathbf{x},\mathbf{s}) e^{i\omega\tau_0} \int dx_2 exp(i\omega x_2^2\tau_{,22}/2)|_0 \ . \tag{24}$$

The integral over x_2 can be evaluated using the formula (eg. Bender and Orszag, 1978)

$$\int d_2x exp(i\omega x_2^2\tau_{,22}|_0)) = e^{i\pi/4}2^{3/2}\pi^{1/2}(\tau_{,22}|_0)^{-1/2} \ . \tag{25}$$

The factor in (25) alters the phase and amplitude to compensate for out-of-plane scattering. The scattering formulae can then be written explicitly (omitting the constant $2^{3/2}\pi^{1/2}$) for individual qP-qP, qP-qS1, $qS1$-qP and qSn-qSn contributions as

$$U_{jk}^{PP} \approx -\omega^{3/2}e^{i\pi/4}\int d\mathbf{x}\left[c'_{lmpq}(\tilde{\alpha}\hat{\alpha})^{-1}\hat{n}_m\tilde{n}_q\hat{e}_l^3\tilde{e}_p^3 - \rho'\delta_{lp}\hat{e}_l^3\tilde{e}_p^3\right](\tau_{,22})^{-1/2}$$
$$\times A^{PP}(\mathbf{r},\mathbf{x},\mathbf{s})\hat{e}_k^3(\mathbf{r})\tilde{e}_j^3(\mathbf{s})e^{i\omega\tau PP(r,x,s)} \quad , \tag{26}$$

$$U_{jk}^{PS} \approx -\omega^{3/2}e^{i\pi/4}\int d\mathbf{x}\left[c'_{lmpq}(\tilde{\alpha}\hat{\beta})^{-1}\hat{n}_m\tilde{n}_q\hat{e}_l^1\tilde{e}_p^3 - \rho'\delta_{lp}\hat{e}_l^1\tilde{e}_p^3\right](\tau_{,22})^{-1/2}$$
$$\times A^{PS}(\mathbf{r},\mathbf{x},\mathbf{s})\hat{e}_k^1(\mathbf{r})\tilde{e}_j^3(\mathbf{s})e^{i\omega\tau PS(r,x,s)} \quad , \tag{27}$$

$$U_{jk}^{SP} \approx -\omega^{3/2}e^{i\pi/4}\int d\mathbf{x}\left[c'_{lmpq}(\tilde{\beta}\hat{\alpha})^{-1}\hat{n}_m\tilde{n}_q\hat{e}_l^3\tilde{e}_p^1 - \rho'\delta_{lp}\hat{e}_l^3\tilde{e}_p^1\right](\tau_{,22})^{-1/2}$$
$$\times A^{SP}(\mathbf{r},\mathbf{x},\mathbf{s})\hat{e}_k^3(\mathbf{r})\tilde{e}_j^1(\mathbf{s})e^{i\omega\tau SP(r,x,s)} \quad , \tag{28}$$

and

$$U_{jk}^{SnSn} \approx -\omega^{3/2} e^{i\pi/4} \int d\mathbf{x} \left[c'_{lmpq} (\beta\beta)^{-1} \hat{n}_m \tilde{n}_q \hat{e}_l^n \tilde{e}_p^n - \rho' \delta_{lp} \hat{e}_l^n \tilde{e}_p^n \right] (\tau_{,22})^{-1/2}$$
$$\times A^{SnSn}(\mathbf{r},\mathbf{x},\mathbf{s}) \hat{e}_k^n(\mathbf{r}) \tilde{e}_j^n(\mathbf{s}) e^{i\omega\tau SnSn(r,x,s)} \quad , \tag{29}$$

where

$$A^{PP}(\mathbf{r},\mathbf{x},\mathbf{s}) \equiv A^P(\mathbf{x},\mathbf{s}) A^P(\mathbf{r},\mathbf{x}) \ , \tag{30}$$

$$A^{PS}(\mathbf{r},\mathbf{x},\mathbf{s}) \equiv A^P(\mathbf{x},\mathbf{s}) A^{SI}(\mathbf{r},\mathbf{x}) \ , \tag{31}$$

$$A^{SP}(\mathbf{r},\mathbf{x},\mathbf{s}) \equiv A^{SI}(\mathbf{x},\mathbf{s}) A^P(\mathbf{r},\mathbf{x}) \ , \tag{32}$$

$$A^{SnSn}(\mathbf{r},\mathbf{x},\mathbf{s}) \equiv A^{Sn}(\mathbf{x},\mathbf{s}) A^{Sn}(\mathbf{r},\mathbf{x}) \ , \text{ (no sum over } n) \tag{33}$$

and

$$\tau^{PP}(\mathbf{r},\mathbf{x},\mathbf{s}) \equiv \tau^P(\mathbf{x},\mathbf{s}) + \tau^P(\mathbf{r},\mathbf{x}) \ , \tag{34}$$

$$\tau^{PS}(\mathbf{r},\mathbf{x},\mathbf{s}) \equiv \tau^P(\mathbf{x},\mathbf{s}) + \tau^{SI}(\mathbf{r},\mathbf{x}) \ , \tag{35}$$

$$\tau^{SP}(\mathbf{r},\mathbf{x},\mathbf{s}) \equiv \tau^{SI}(\mathbf{x},\mathbf{s}) + \tau^P(\mathbf{r},\mathbf{x}) \ , \tag{36}$$

$$\tau^{SnSn}(\mathbf{r},\mathbf{x},\mathbf{s}) \equiv \tau^{Sn}(\mathbf{x},\mathbf{s}) + \tau^{Sn}(\mathbf{r},\mathbf{x}) \ . \text{ (no sum over } n) \tag{37}$$

Note that both the stationary phase approximation and the ray approximation to the elastodynamic Green's functions represent high-frequency asymptotic parts of the full solution, and hence are mutually compatible approximations. This approach significantly reduces the computational overhead, by permitting 2-D, rather than 3-D generation of background Green's functions.

WEAK TRANSVERSE ISOTROPY

The special case of a transversely isotropic medium with a vertical axis of symmetry (TIV) is now considered. This special case can easily be generalized to permit any orientation of the symmetry axis within the sagittal plane. For a TIV medium, the 6×6 stress matrix has the form

$$\mathbf{C} = \begin{bmatrix} C_{11} & C_{12} & C_{13} & 0 & 0 & 0 \\ C_{12} & C_{11} & C_{13} & 0 & 0 & 0 \\ C_{13} & C_{13} & C_{33} & 0 & 0 & 0 \\ 0 & 0 & 0 & C_{44} & 0 & 0 \\ 0 & 0 & 0 & 0 & C_{44} & 0 \\ 0 & 0 & 0 & 0 & 0 & C_{66} \end{bmatrix} , \tag{38}$$

where $C_{12} = C_{11} - 2C_{66}$. The relationship between the elements of the stress matrix, C_{ij}, and the 21 nonzero elements of the corresponding stress tensor, c_{lmpq}, is summarized in Table 1. Noting that for rays within the sagittal plane, $\tilde{e}_i^2 = \hat{e}_i^2 = 0$, $i = 1,2,3$, for qP and $qS1$ waves and $\tilde{e}_1^2 = \tilde{e}_3^2 = \hat{e}_1^2 = \hat{e}_3^2 = 0$ for $qS2$ waves, the vector $\mathbf{s}^{ls}$ for a TIV medium may be written

$$\mathbf{s}^{PP} = (\tilde{\alpha}\hat{\alpha})^{-1}\big(\hat{n}_1\tilde{n}_1\hat{e}_1^3\tilde{e}_1^3,\ \hat{n}_3\tilde{n}_3\hat{e}_3^3\tilde{e}_3^3,\ \hat{n}_1\tilde{n}_3\hat{e}_1^3\tilde{e}_3^3+\hat{n}_3\tilde{n}_1\hat{e}_3^3\tilde{e}_1^3,\ \hat{n}_1\tilde{n}_1\hat{e}_3^3\tilde{e}_3^3+\hat{n}_3\tilde{n}_3\hat{e}_1^3\tilde{e}_1^3+ \\ \hat{n}_1\tilde{n}_3\hat{e}_3^3\tilde{e}_1^3+\hat{n}_3\tilde{n}_1\hat{e}_1^3\tilde{e}_3^3,\ 0,\ -(\tilde{\alpha}\hat{\alpha})\cos\theta^{PP}\big)^{\mathrm{T}} , \tag{39}$$

$$\mathbf{s}^{PS} = (\tilde{\alpha}\beta)^{-1}\big(\hat{n}_1\tilde{n}_1\hat{e}_1^1\tilde{e}_1^3,\ \hat{n}_3\tilde{n}_3\hat{e}_3^1\tilde{e}_3^3,\ \hat{n}_1\tilde{n}_3\hat{e}_1^1\tilde{e}_3^3+\hat{n}_3\tilde{n}_1\hat{e}_3^1\tilde{e}_1^3,\ \hat{n}_1\tilde{n}_1\hat{e}_3^1\tilde{e}_3^3+\hat{n}_3\tilde{n}_3\hat{e}_1^1\tilde{e}_1^3+ \\ \hat{n}_1\tilde{n}_3\hat{e}_3^1\tilde{e}_1^3+\hat{n}_3\tilde{n}_1\hat{e}_1^1\tilde{e}_3^3,\ 0,\ -(\tilde{\alpha}\beta)\cos\theta^{PS}\big)^{\mathrm{T}} , \tag{40}$$

$$\mathbf{s}^{SP} = -\mathbf{s}^{PS} , \tag{41}$$

$$\mathbf{s}^{S1\text{-}S1} = (\tilde{\beta}\hat{\beta})^{-1}\big(\hat{n}_1\tilde{n}_1\hat{e}_1^1\tilde{e}_1^1,\ \hat{n}_3\tilde{n}_3\hat{e}_3^1\tilde{e}_3^1,\ \hat{n}_1\tilde{n}_3\hat{e}_1^1\tilde{e}_3^1+\hat{n}_3\tilde{n}_1\hat{e}_3^1\tilde{e}_1^1, \hat{n}_1\tilde{n}_1\hat{e}_3^1\tilde{e}_3^1+\hat{n}_3\tilde{n}_3\hat{e}_1^1\tilde{e}_1^1+ \\ \hat{n}_1\tilde{n}_3\hat{e}_3^1\tilde{e}_1^1+\hat{n}_3\tilde{n}_1\hat{e}_1^1\tilde{e}_3^1,\ 0,\ -(\tilde{\beta}\hat{\beta})\cos\theta^{SS}\big)^{\mathrm{T}} , \tag{42}$$

and

$$\mathbf{s}^{S2\text{-}S2} = (\tilde{\beta}\hat{\beta})^{-1}\big(0,\ 0,\ 0,\ \hat{n}_3\tilde{n}_3,\ \hat{n}_1\tilde{n}_1,\ -(\tilde{\beta}\hat{\beta})\big)^{\mathrm{T}} , \tag{43}$$

where

$$\mathbf{m}^1 = (C_{11}, C_{33}, C_{13}, C_{44}, C_{66}, \rho)^{\mathrm{T}} , \tag{44}$$

and θ^{ls} is the angle subtended by the particle-motion vector for the incident and scattered rays. For the degenerate case of complete isotropy, $C_{11} = C_{33} = \lambda+2\mu$, $C_{44} = C_{66} = \mu$ and $C_{13} = \lambda$, where λ and μ are the lamé parameters. After some algebra, the scattering vector can then be written

$$\mathbf{s}^{PP} = (\alpha^0)^{-2}(1,\ 2\cos^2\phi^{PP},\ (\alpha^0)^2\cos\phi^{PP})^{\mathrm{T}} , \tag{45}$$

$$\mathbf{s}^{PS} = (\alpha^0\beta^0)^{-1}(0,\ \sin 2\phi^{PS},\ \alpha^0\beta^0\sin\phi^{PS})^{\mathrm{T}} , \tag{46}$$

$$\mathbf{s}^{SP} = -\mathbf{s}^{PS} , \tag{47}$$

$$\mathbf{s}^{SV\text{-}SV} = (\beta^0)^{-2}(0,\ \cos 2\phi^{SS},\ (\beta^0)^2\cos\phi^{SS})^{\mathrm{T}} , \tag{48}$$

and

Table 1. Stress tensor for TIV medium

c_{lmpq}	C_{ij}
c_{1111}	C_{11}
c_{2222}	C_{11}
c_{3333}	C_{33}
c_{1122}	C_{11}-$2C_{66}$
c_{2211}	C_{11}-$2C_{66}$
c_{1133}	C_{13}
c_{2233}	C_{13}
c_{3311}	C_{13}
c_{3322}	C_{13}
c_{3232}	C_{44}
c_{2323}	C_{44}
c_{3223}	C_{44}
c_{2332}	C_{44}
c_{3131}	C_{44}
c_{1313}	C_{44}
c_{3113}	C_{44}
c_{1331}	C_{44}
c_{1212}	C_{66}
c_{2121}	C_{66}
c_{1221}	C_{66}
c_{2112}	C_{66}

$$\mathbf{s}^{SH\text{-}SH} = (\beta^0)^{-2}(0,\ \cos\phi^{SS},\ (\beta^0)^2)^T\ , \tag{49}$$

where in this case the reference model parameter vector is

$$\mathbf{m}^1 = (\lambda,\ \mu,\ \rho)^T\ . \tag{50}$$

and ϕ is the angle subtended by the incident and scattered rays. The only aspect of the ray geometry that plays a role in scattering for the isotropic case is the angle between the incident and scattered rays. In the anisotropic case, the scattering also depends on the angle that each of these rays makes with the axis of symmetry. Thus, although more parameters are required to describe the model, the scattered energy also carries more information about the medium.

For modeling and inversion using the reference model parameters, the matrix **L** takes the simple form

$$L_{lp} = \delta_{lp}\ \ . \tag{51}$$

However, because the elastic stiffnesses are an inconvenient parameterization for most geophysicists, it is desirable to change to a more intuitive set of model parameters. For the case of a TIV medium, a useful alternative parameterization is given by

$$\mathbf{m}^2 = (\alpha_v, \beta_v, \delta, \varepsilon, \gamma, \rho)^T \quad , \tag{52}$$

where the first five parameters are defined (Thomsen, 1986)

$$\alpha_v \equiv (C_{33}/\rho)^{1/2} \, , \tag{53}$$

$$\beta_v \equiv (C_{44}/\rho)^{1/2} \, , \tag{54}$$

$$\delta \equiv [(C_{13} + C_{44})^2 - (C_{33} - C_{44})^2][2C_{33}(C_{33} - C_{44})]^{-1} \, , \tag{55}$$

$$\varepsilon \equiv (C_{11} - C_{33})(2C_{33})^{-1} \, , \tag{56}$$

and

$$\gamma \equiv (C_{66} - C_{44})(2C_{44})^{-1} \, . \tag{57}$$

For this parameterization, the matrix **L** can be written (for an isotropic background) as

$$\mathbf{L}^2 = \begin{bmatrix} 2\alpha_v^0\rho^0 & 0 & 0 & 2(\alpha_v^0)^2\rho^0 & 0 & (\alpha_v^0)^2 \\ 2\alpha_v^0\rho^0 & 0 & 0 & 0 & 0 & (\alpha_v^0)^2 \\ 2\alpha_v^0\rho^0 & -4\beta_v^0\rho^0 & (\alpha_v^0)^2\rho^0 & 0 & 0 & (\alpha_v^0)^2-2(\beta_v^0)^2 \\ 0 & 2\beta_v^0\rho^0 & 0 & 0 & 0 & (\beta_v^0)^2 \\ 0 & 2\beta_v^0\rho^0 & 0 & 0 & 2(\beta_v^0)^2\rho^0 & (\beta_v^0)^2 \\ 0 & 0 & 0 & 0 & 0 & 1 \end{bmatrix} . \tag{58}$$

l_2-NORM INVERSION

It is possible to cast the inversion as an l_2-norm optimization problem. A general objective function can be defined (Tarantola, 1987)

$$E = 1/2\left(\delta\mathbf{u}^*\cdot\mathbf{C}_u^{-1}\cdot\delta\mathbf{u} + \delta\mathbf{m}^*\cdot\mathbf{C}_m^{-1}\cdot\delta\mathbf{m}\right) \quad , \tag{59}$$

where $\delta\mathbf{u}$ and $\delta\mathbf{m}$ are data and model residual vectors, $\mathbf{C}_u$ and $\mathbf{C}_m$ are *a priori* covariance operators associated with the data and model, respectively, and * denotes conjugate transpose. In the Born approximation, we have

$$\delta\mathbf{u} = \mathbf{u}_{obs} - \mathbf{B}\cdot\delta\mathbf{m} \quad , \tag{60}$$

where **B** is the Born operator. The gradient of the objective function, $\partial E/\partial\mathbf{m}$ is

$$\nabla E = -\mathbf{B}^*\cdot\mathbf{C}_u^{-1}\cdot\delta\mathbf{u} + \mathbf{C}_m^{-1}\cdot\delta\mathbf{m} \quad . \tag{61}$$

A vector pointing in the steepest-descent direction (establishing a line of search for updating the model) is $-\nabla E$. The model update can then be written

$$\delta \mathbf{m} = \sigma(-\nabla E) \quad . \tag{62}$$

The step length, σ, is found by an independent single-parameter search. Following LeBras and Clayton (1988), the backprojection operator B^* can be determined by first defining the inner product of two vector **x** and **y** in V as

$$\langle \mathbf{x},\mathbf{y} \rangle = \int dV \, \mathbf{x}^* \mathbf{y} \quad . \tag{63}$$

The backprojection operator, $\mathbf{B}^*$, is then fully defined by

$$\langle \delta \mathbf{u}, \mathbf{B} \cdot \delta \mathbf{m} \rangle = \langle \mathbf{B}^* \cdot \delta \mathbf{u}, \delta \mathbf{m} \rangle \quad . \tag{64}$$

The operator $\mathbf{B}^*$ acts as a filtered backprojection of the data. Inclusion of the model covariances in the objective function acts as a damping term to ensure that the invsersion does not diverge too far from the initial model, and also to ensure that the problem is always well-posed (Tarantola, 1987).

CONCLUSIONS

A method has been outlined for performing migration/inversion for transversely isotropic media. The algorithm accounts for both differences in wave *propagation* and *scattering* caused by anisotropy. Incorporation of anisotropy may result in improved subsurface images for some areas. Furthermore, inversion for the anisotropic parameters (δ, ε and γ) may assist in discrimination between sands and shales, analysis of periodic thin layering and fracture detection.

Several important observations can be noted concerning the form of the scattering functions for a TIV medium, and the potential for Born inversion algorithms:

1) In order to obtain all 5 elastic parameters plus density using 2-D data, 3-component sources and receivers are required. Using P-SV data, at most 4 out of the 5 elastic parameters are resolvable.

2) Only P-P scattering is sensitive to perturbations in the parameter α_v; only SH-SH scattering is sensitive to changes in the parameter γ.

3) In the zero-offset case, mode-converted backscattered energy is possible, due to perturbations in the anisotropic parameters.

4) For the isotropic case, the angle-dependent parameters in the scattering functions depend only on the angle subtended between the source and receiver rays. For the anisotropic case, the scattering function depends also on the absolute direction of the incident and scattered rays with respect to the axis of symmetry of the anisotropic medium (in this case, vertical).

It is well known that in the absence of a wide range of offsets, multiparameter seismic inversion (isotropic) is non-unique. Intuitively, adding more parameters should compound the non-uniqueness problem. However, point 4 above suggests that perhaps for anisotropic scattering, the additional information conveyed by the raypath geometry will partially offset the non-uniqueness problem.

ACKNOWLEDGMENTS

We would like to express our thanks to the sponsors of the CREWES project at the University of Calgary. The first author (DE) would also like to thank Wafik Beydoun, Ali Tura and Arthur Weglein at Arco Research and Technical Services for their suggestions and discussion of this material.

REFERENCES

Bender, C.M., and Orszag, S.A., 1978, Advanced mathematical methods for scientists and engineers: McGraw-Hill Book Co.

Beydoun, W.B., and Mendes, M., 1989, Elastic ray-Born l_2-migration/inversion: Geophys. J. Int., 97, 151-160.

Beydoun, W.B., Delvaux, J., Mendes, M., Noual, G., and Tarantola, A., 1989, Practical aspects of an elastic migration/inversion of crosshole data for reservoir characterization: A Paris basin example: Geophysics, 54, 1587-1595.

Beydoun, W.B., Mendes, M., Blanco, J., and Tarantola, A., 1990, North Sea reservoir description: Benefits of an elastic migration/inversion applied to multicomponent vertical seismic profile data: Geophysics, 55, 209-217.

Beylkin, G. 1985, Imaging of discontinuities in the inverse scattering problem by inversion of a causal generalized Radon transform: J. Math. Phys., 26, 99-108.

Beylkin, G., and Burridge, R., 1990, Linearized inverse scattering problems in acoustics and elasticity: Wave Motion, 12, 15-52.

Bleistein, N., 1986, Two-and-one-half dimensional in-plane wave propagation: Geophys. Prosp., 34, 686-703.

Bleistein, N., and Gray, S.H., 1985, An extension of the Born inversion method to a depth dependent reference profile: Geophys. Prosp., 33, 999-1022.

Bleistein, N., Cohen, J.K., and Hagin, F.G., 1985, Computational and asymptotic aspects of velocity inversion: Geophysics, 50, 1253-1265.

Bleistein, N., Cohen, J.K., and Hagin, F.G., 1987, Two and on-half dimensional Born inversion with an arbitrary reference: Geophysics, 52, 26-36.

Clayton, R.W., and Stolt, R.H., 1981. A Born-WKBJ inversion method for acoustic reflection data: Geophysics, 46, 1559-1567.

Cohen, J.K., and Bleistein, N., 1979, Velocity inversion procedure for acoustic waves: Geophysics, 44, 1077-1087.

Cohen, J.K., Hagin, f.G., and Bleistein, N., 1986, Three-dimensional Born inversion with an arbitrary reference: Geophysics, 51, 1552-1558.

Crampin, S., Chesnokov, E.M., and Hipkin, R.A., 1984, Seismic anisotropy - the state of the art: Geophys. J. Roy. Astr. Soc., 76, 1-16.

LeBras, R., and Clayton, R.W., 1988, An iterative inversion of back-scattered acoustic waves: Geophysics, 53, 501-508.

Miller, D., Oristaglio, M., and Beylkin, G., 1987, A new slant on seismic imaging: Migration and integral geometry: Geophysics, 52, 943-964.

Musgrave, M.J.P., 1970, Crystal Acoustics: Introduction to the study of elastic waves and vibrations in crystals: Holden-Day.

Newton, R.G., 1966, Scattering theory ow waves and particles: McGraw-Hill Book Co.

Raz, S., 1981, Direct reconstruction of velocity and density profiles from scattered field data: Geophysics, 46, 832-836.

Snieder, R., 1990, A perturbative analysis of non-linear inversion: Geophys. J. Int., 101, 545-556.

Tarantola, A., 1986, A strategy for nonlinear elastic inversion of seismic reflection data: Geophysics, 51, 1893-1903.

Tarantola, A., 1987, Inverse problem theory: Methods for data fitting and model parameter estimation: Elsevier.

Thomsen, L., 1986, Weak elastic anisotropy: Geophysics, 51, 1954-1966.

Tura, M.A.C., 1990, Acoustic and elastic diffraction tomography and its application to fracture detection. Ph.D. thesis, University of California at Berkeley, 182 pp.

Weglein, A.B., Violette, P.B. and Keho, T.H., 1986, Using multiparameter Born theory to obtain certain exact multiparameter inversion goals: Geophysics, 51, 1069-1074.